

# Flow rule, self-channelization and levees in unconfined granular flows.

S. Deboeuf, E. Lajeunesse

*Institut de Physique du Globe de Paris, 4 place Jussieu, 75252 Paris cedex 05, France*

O. Dauchot

*CEA Saclay/SPEC, URA2464, L'Orme des Merisiers, 91 191 Gif-sur-Yvette, France*

B. Andreotti

*Laboratoire de Physique et Mécanique des Milieux Hétérogènes, 10 rue Vauquelin, 75005 Paris, France*

Unconfined granular flows along an inclined plane are investigated experimentally. The flow rule for such unsteady and inhomogeneous flows is obtained and exhibits a crossover toward a non local rheology close to arrest. During a long transient, the flow gets confined by quasi-static banks but still spreads laterally following a non-diffusive process. Upon interruption of the flow, the formation of levees along the sides of the deposit is eventually observed, but they disappear for long flow durations. We demonstrate that the morphology of the deposit builds up *during* the flow, in the form of an underlying static layer, which can be deduced from surface velocity profiles, by imposing the same flow rule everywhere in the flow.

Geophysical granular flows such as debris flows or rock avalanches usually self-channelize, forming a coulee surrounded by static banks, until they come to arrest and form a deposit [1, 2] with levee/channel morphology. Despite recent investigations [3], the formation mechanism of levees remains unclear, and further progress in that matter requires a better knowledge of granular flows rheology. When sufficiently far from the jamming transition, it has been recently shown [4] that the rheology of shear flows is *local*, in first approximation: the shear stress  $\tau$  depends on the shear rate  $\dot{\gamma}$  at the considered point only. It follows from dimensional analysis that the rheology can be expressed under the non-dimensional form  $\tau/P = \mu_I(I)$  with  $I = \dot{\gamma}d/(P/\rho)^{1/2}$ , where  $d$  is the grain diameter,  $P$  the pressure and  $\rho$  the density. This rheology has recently been extended to three dimensions and validated in various flow configurations, including non-steady and non-uniform flows as well as flows on erodible ground [4, 5].

The case of a homogeneous layer of spherical beads, confined between two side walls, flowing down an inclined plane is of particular interest. Experiments and numerical simulations have drawn two important results [4, 6, 7]. First, there is a minimum thickness  $h_{\text{stop}}(\theta)$  below which no flow occurs and a maximum one  $h_{\text{start}}(\theta)$  above which static layers spontaneously destabilise. Second, the flow rule relating the depth averaged velocity  $\bar{u}$  to the thickness  $h$  is consistent with a local rheology and obeys

$$\frac{\bar{u}}{\sqrt{gh}} = \beta \frac{h}{h_{\text{stop}}(\theta)}, \quad (1)$$

where  $g$  is the gravity and  $\beta$  a non-dimensional parameter dependent on the grains. However, the flow rule (1) does not verify  $\bar{u}(h_{\text{stop}}) = 0$ , and hence does not encode the flow arrest. Besides  $h_{\text{stop}}(\theta)$  and  $h_{\text{start}}(\theta)$  are obviously non-local jamming/unjamming conditions. Hence, it is of primary importance, both for practical and fundamental

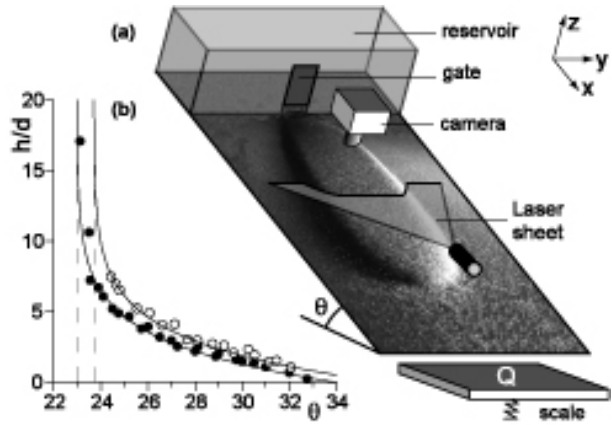


FIG. 1: (a) Sketch of the experimental setup. (b) Phase diagram in the plane  $(h/d, \theta)$ : the experimental data for  $h_{\text{stop}}(\theta)$  (●) and  $h_{\text{start}}(\theta)$  (○) with the best fits by eq. (2) (solid line).

reasons, to study a situation where flowing and static regions coexist. In this letter, we study experimentally an *unconfined* avalanche down an inclined plane. By contrast to the homogeneous case, the flow self-channelizes within static banks which may evolve freely. Our main aims are to characterise the dynamics of the flow on the one hand, and its relation to the morphology of the deposit when the flow stops on the other hand.

*Set-up* – The experimental setup is sketched on Fig. 1(a). A  $60 \times 300 \text{ cm}^2$  plane, covered with sand paper of average roughness about  $200 \mu\text{m}$ , is inclined at an angle  $\theta$  ranging from  $24^\circ$  to  $34^\circ$ . The granular material consists of a slightly polydisperse mixture of spherical glass beads of diameter  $d = 350 \pm 50 \mu\text{m}$  and density  $\rho = 2500 \text{ kg.m}^{-3}$ . Grains are released from a reservoir located at the top of the plane by opening a gate of adjustable height and width. To produce homogeneous flows, the whole plane width is used, but for unconfined flows the gate width is reduced to 5 cm and the width of the plane is always larger than that of the avalanche. In

the case of homogeneous flows, the standard phase diagram is recovered (Fig. 1b),  $h_{\text{start}}(\theta)$  and  $h_{\text{stop}}(\theta)$  obey

$$\tan \theta = \mu^\infty + (\mu^0 - \mu^\infty) \exp(-h/\alpha d), \quad (2)$$

with  $\alpha = 3.2$ ,  $\theta_{\text{stop}}^\infty = 22.5^\circ$ ,  $\theta_{\text{start}}^\infty = 23.0^\circ$ ,  $\theta_{\text{stop}}^0 = 33.6^\circ$ , and  $\theta_{\text{start}}^0 = 35.6^\circ$ . The mass flow rate  $Q$  is measured at the end of the plane, where the grains fall inside a reservoir resting on a scale. During all experiments, some of which lasted up to 5 h,  $Q$  fluctuated by less than 2%. A  $572 \times 768$  pixels camera positioned at the vertical of the plane is used to acquire images of the flow at 25 Hz. The deviation of a laser sheet illuminating the surface of the layer with a very low incident angle allows us to measure the local flow thickness with an accuracy of  $60 \mu\text{m}$ . About 10% of the grains are coloured in black and the velocity of the surface grains,  $u_s$ , is measured using a particle-imaging velocimetry algorithm. In all experiments the spanwise velocity component is found to be smaller than the resolution (2 mm/s).

*Flow rule* – The flow rule is first determined using homogeneous steady flows covering the total width of the plane (Fig. 2a). For  $h/h_{\text{stop}} > 2$  it is consistent with a local rheology and the best fit by eq. (1) gives  $\beta = 0.134$  assuming  $\bar{u}/u_s = 3/5$  (see below). However for thinner thickness, there is a small but systematic deviation toward lower value of the velocity. This tiny indication of a violation of the local rheology close to jamming is confirmed by the measurement of the ratio of the depth averaged velocity  $\bar{u}$  – measured with the avalanche front velocity – to the surface velocity  $u_s$  (Fig. 1c). While it is consistent with the Bagnolds-like profile deriving from a local rheology [4] whose signature is  $\bar{u}/u_s = 3/5$ , for large values of  $h/h_{\text{stop}}$ ,  $\bar{u}/u_s$  decreases to  $1/2$  close to the jamming transition, in agreement with numerical findings [8] of a transition toward a linear velocity profile. Self-channelized flows are naturally very thin so that they give us access precisely to the range of thickness that is difficult to explore in the case of homogeneous flows. In this former case, upon release of the grains, an avalanche front propagates down the plane at a constant velocity, leaving behind it a streamwise homogeneous flow (Fig. 1a). Fig. 2(b) shows data collected near the centerline of the flow, where both the transverse slope  $\partial_y h$  and the rescaled curvature  $h\partial_{yy}h$  are small. Plotting  $u_s/\sqrt{gh}$  as a function of  $h/h_{\text{stop}}$ , one observes again a collapse of data (for different  $\theta$ ,  $Q$  and  $t$ ) on a single curve well fitted by

$$\frac{\bar{u}}{\sqrt{gh}} = \tilde{\beta} \left( \frac{h}{h_{\text{stop}}(\theta)} - 1 \right), \quad (3)$$

with  $\tilde{\beta} = 0.219$  assuming now  $\bar{u}/u_s = 1/2$ . The same fit reported on the data for the homogeneous flow case (Fig. 2a) coincides with the points escaping the usual scaling. Altogether our measurements provide – to the best of our knowledge – the first experimental determination of the flow rule over the whole range of thickness. It

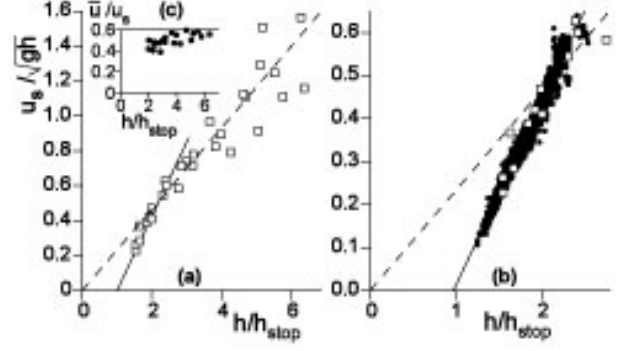


FIG. 2: Flow rule:  $u_s/(gh)^{1/2}$  vs  $h/h_{\text{stop}}$ . (a) Data for steady homogeneous flows ( $\square$ ). (b) Data obtained in the central – quasi-homogeneous – part of unconfined flows ( $\bullet$ ). The solid (resp. dashed) line is the best fit by eq. (3) (resp. eq. (1)). (c) Average to surface velocity ratio  $\bar{u}/u_s$  vs.  $h/h_{\text{stop}}$ .

consists in eqs. (1) and (3) linked by a crossover close to  $h/h_{\text{stop}} = 2$ . It clearly shows that the rheology becomes non-local when approaching the jamming transition and it is compatible with  $\bar{u}(h_{\text{stop}}) = 0$ .

*Transverse spreading* – Fig. 3(a) displays thickness profiles at successive time steps. It shows that the flow widens while the thickness profiles bend progressively. The flow thickness converges rapidly toward an asymptotic value  $H_\infty(\theta, Q)$ , whereas its width converges to an asymptotic value  $W_\infty(\theta, Q)$  with a much larger relaxation time (Fig. 3b). When preparing a flow of width larger than  $W_\infty$  by increasing the flow rate, and returning to the initial flow rate, the width decreases back to  $W_\infty$ . This puts beyond any doubt the existence of a self-channelization. Both the asymptotic width  $W_\infty$  and height  $H_\infty$  are observed to increase with the flow rate  $Q$ . The aspect ratio  $H_\infty/W_\infty$  turns out to be independent of  $Q$  and slightly decreases with  $\theta$  (Fig. 3c). From conservation of mass, one expects a linear relation between  $Q$  and  $H_\infty W_\infty \bar{u}(H_\infty) \propto \rho g^{1/2} H_\infty^{5/2} (H_\infty/h_{\text{stop}} - 1)$ , using eq. (3). This relation is closely verified experimentally (Fig. 3d).

It is interesting to compare this evolution to that predicted by the St-Venant equations [9]. We assume that the flow only depends on time  $t$  and on the transverse coordinate  $y$ . Inertia being negligible, the mass balance and the force equilibrium simplify into

$$\partial_t h + \partial_y(\bar{u}_y h) = 0 \quad (4)$$

$$\tan \theta \vec{e}_x - \partial_y h \vec{e}_y - \mu_I(\bar{u}, h) \frac{\vec{u}}{\bar{u}} = \vec{0}. \quad (5)$$

Accordingly the free surface slope  $\tan \Phi \equiv (\tan^2(\theta) + (\partial_y h)^2)^{1/2}$  is equal to  $\mu_I$  and the height  $h$  is governed by a non-linear diffusion equation

$$\partial_t h = \partial_y(D \partial_y h) \text{ with } D = \bar{u} h / \mu_I(\bar{u}, h), \quad (6)$$

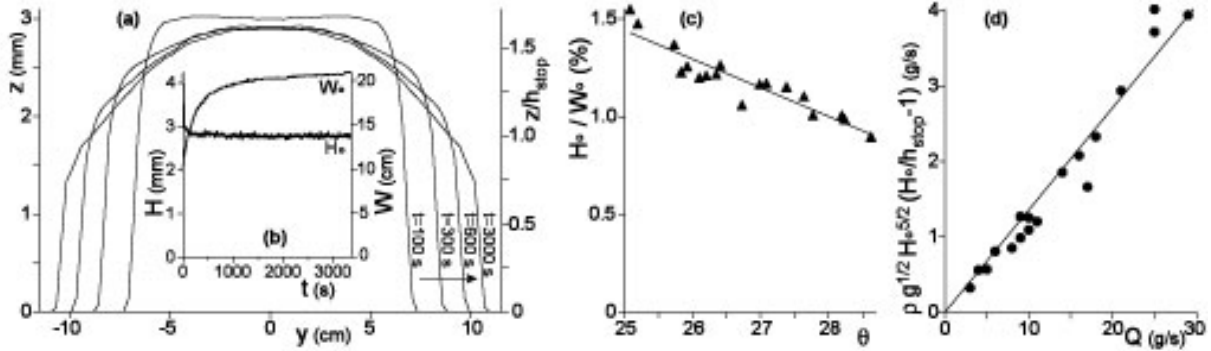


FIG. 3: (a) Time evolution of the height profiles  $h(y, t)$  for  $Q = 25 \text{ g.s}^{-1}$ ,  $\theta = 25^\circ$ . (b) Evolution of the height  $H$  and width  $W$  of the flow. (c) Asymptotic aspect ratio of the flow  $H_\infty/W_\infty$  as a function of the slope angle. (d) Scaling of the asymptotic height with the flow rate:  $\rho g^{1/2} H^{5/2} (H_\infty/h_{\text{stop}} - 1)$  as a function of  $Q$ .

whose diffusion time scales as  $W^2/\bar{u}H$ , which may explain the surprisingly slow relaxation of  $W$ . However, following such a diffusive dynamics, the asymptotic steady behaviour would be expected to be flat ( $\partial_y h = 0$ ) in the inner flowing region ( $\bar{u} \neq 0$ ) as the diffusion coefficient  $D$  is not zero there. This is not the case experimentally as the free surface becomes more and more curved as time goes by (Fig. 3a). Such a behaviour cannot be explained unless the normal stress  $\tau_{yy}$  in the transverse direction  $y$  depends on the transverse velocity gradient  $|\partial_y u_x|$ . This abnormal behaviour, which exists in suspensions, has never been evidenced in dense granular flows. Note that the temporal scalings of both  $W(t)$  and  $H(t)$  derived from eq. (6) also disagree with the experimental observations [10].

*Banks* – Fig. 4(a) shows the transverse structure of the avalanche: the inner flowing region ( $u \neq 0$ ) is flanked by two static banks ( $u = 0$ ) of width approximately 5 mm. Also the external side of these banks is rather steep so that the free surface angle  $\Phi$  becomes significantly larger than the plane angle  $\theta$  (Fig. 4b). It can be observed that the banks, although quasi-static, are outside the metastable band  $[h_{\text{stop}}, h_{\text{start}}]$  during the spreading phase but converge toward it in the asymptotic state – the external part of the banks then follows the curve  $h = h_{\text{stop}}(\Phi)$ . In the previous section we investigated the flow rule near the centerline of the flow. No such scaling is *a priori* expected close to the static banks. Indeed as seen on Fig. 4(d), when acquiring data moving away from the centerline, no scaling is observed and the surface velocity  $u_s$  is systematically underestimated. A possible explanation of such a deviation from the otherwise scaling is the extension of the static zone below the flowing grains. In order to verify such an hypothesis, we performed specific experiments. One first conducts an experimental run using white grains. After a few minutes, the flow is stopped and a deposit forms. The white grains of a small slice across the deposit are removed and replaced by black grains of the same material. The flow is then started again at the same flow rate. At the surface, the

black grains are washed out by the incoming white grains except in the static borders. After a few minutes, the flow is interrupted again. Using a brush, the white grains are removed very cautiously layer after layer in the region of the slice. Close to the centre, the deposit is exclusively composed of the new white grains, proving that the flow involves the whole thickness. However, close to

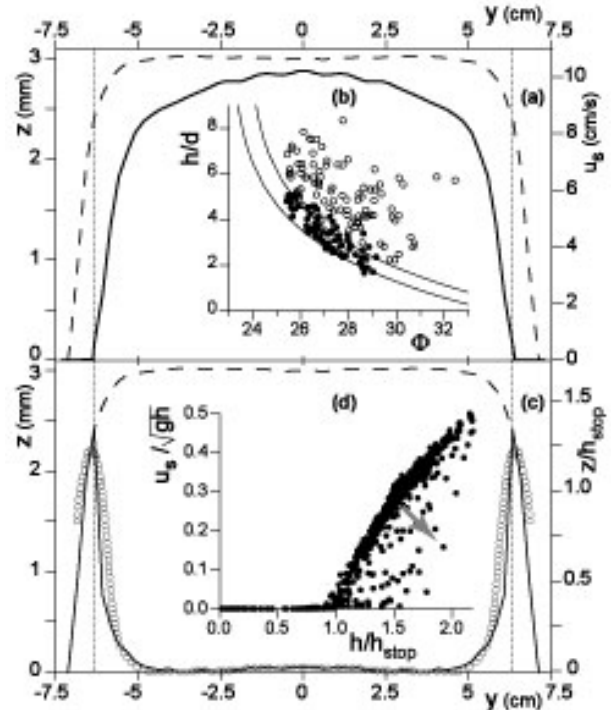


FIG. 4: (a) Velocity  $u(y)$  (solid line) and thickness  $h(y)$  (dashed line) profiles for  $\theta = 25^\circ$ ,  $Q = 25 \text{ g.s}^{-1}$  and  $t = 150 \text{ s}$ . (b) Thickness vs. local slope  $\Phi$  inside the quasi-static banks ( $\circ$ :  $t < 2000 \text{ s}$ ,  $\bullet$ : asymptotic state). The solid lines show  $h_{\text{stop}}$  and  $h_{\text{start}}$ . (c) Static layer thickness  $Z$  reconstructed from surface velocity measurements (solid line) and directly measured with a brush ( $\circ$ ). (d)  $u_s/(gh)^{1/2}$  vs  $h/h_{\text{stop}}$ : the existence of a static layer results in a progressive shift from the flow rule when moving away from the centerline (arrow).

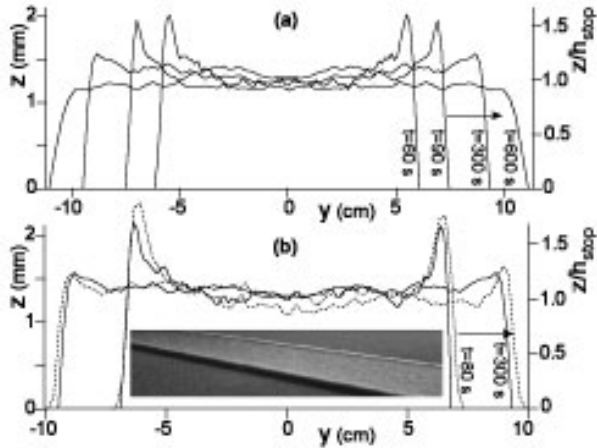


FIG. 5: (a) Thickness profiles of the deposit  $h_{\text{dep}}(y)$  obtained after different flow durations for  $Q = 25 \text{ g.s}^{-1}$ ,  $\theta = 26^\circ$ . (b) Comparison between measured (solid line) and predicted (dotted line) deposit profiles.

the banks, a layer of black grains remained trapped, indicating the presence of a static layer of thickness  $Z(y, t)$  (denoted by  $\circ$  in Fig. 4c) below the flowing one. Using  $u_s$ , one can construct the thickness  $R \leq h$  which would flow if the flow rule obtained above were applicable inside the flowing layer. The reconstructed static/flowing interface  $Z = h - R$  is shown on Fig. 4(c) together with the real one. One can see that the agreement is fairly good. It suggests that, to the first order, the grains flow on the static grains just like they flow on the rough plane. At the same order, it tells us that the flow rule is actually observed everywhere in the flow when applied to the flowing thickness  $R$  instead of the total one  $h$ .

*Levees* – Turn now to the morphology of the deposit which forms when the flow stops. It has been reported [3] that, under certain conditions of inclination and flow rate, the deposit formed upon interruption of the flow exhibits a levee/channel morphology similar to those observed on pyroclastic flow deposits. In the present study, we have shown that for larger times, the flow actually keeps on widening and converges only very slowly toward its asymptotic state. Accordingly the shape of the deposit strongly depends on the flow duration  $t$  (Fig. 5a). For small  $t$ , deposits are composed of a central flat zone of thickness  $h_{\text{stop}}$  bordered by two levees of thickness larger than  $h_{\text{stop}}$  as previously reported [3]. When  $t$  increases, the levee thicknesses decrease until they vanish at very long time, so that the deposit corresponding to the asymptotic state is indeed flat. Levees result from the combination between lateral static zones on each border

of the flow and the drainage of the central part of the flow after the supply stops. However, a clear picture is still lacking concerning the junction between a central flat zone of thickness  $h_{\text{stop}}$  and a levee of thickness larger than  $h_{\text{stop}}$ . The flow rule that was obtained here provides a very simple scenario. The flow stops when  $R = h_{\text{stop}}$ , and one expects the deposit to form by superimposing a layer of thickness  $h_{\text{stop}}$  to the static layer. Accordingly the deposit thickness should be  $h_{\text{dep}} = Z + h_{\text{stop}}$  whenever  $u_s \neq 0$  and  $h_{\text{dep}} = Z$  in the quasi-static banks, where  $u_s = 0$ . Fig 5(b) provides the experimental evidence that such a simple scenario indeed holds: the deposit profile built following the above argument matches perfectly the measured one.

To conclude, by investigating unconfined granular flows along an inclined plane, we have shown that they obey a flow rule which reveals a crossover toward a non local rheology for very thin flows. This flow rule accounts for the the morphology of the deposit, which forms when the flow ceases, and actually builds up *during* the flow, in the form of an underlying static layer. This underlines the importance of addressing erosion-deposition mechanisms issues to complete a full description of geophysical flows.

The authors aknowledge E. Clément, F. Malloggi, J-P. Vilotte for fruitfull discussions and Y. Gamblin for technical assistance.

---

- [1] R.M. Iverson, *Reviews of Geophysics* **35**, 245296 (1997).
- [2] M.A. Hampton, H.J. Lee and J. Locat, *Reviews of Geophysics* **34**, 3359 (1996).
- [3] G. Felix and N. Thomas, *Earth and Planetary Science Letters* **221**, 197 (2004).
- [4] G.D.R. Midi (collective work), *Eur. Phys. Jour. E* **14**, 341 (2004).
- [5] Y. Forterre and O. Pouliquen, *J. Fluid Mech.* **486**, 21 (2003); P. Jop, Y. Forterre and O. Pouliquen, to appear in *Nature* (2006); P. Jop, Y. Forterre and O. Pouliquen, *J. Fluid Mech.* **541**, 167 (2005).
- [6] F. da Cruz, S. Emam, M. Prochnow, J-N. Roux and F. Chevoir, *Phys. Rev. E* **72** 21309 (2005).
- [7] O. Pouliquen, *Phys. Fluids* **11**, 542 and 1956 (1999).
- [8] S.L. Silbert, J.W. Landry and G.S. Grest, *Phys. Fluids* **15**, 1 (2003).
- [9] S.B. Savage and K. Hutter, *J. Fluid Mech.* **199**, 177 (1989).
- [10] In the limit  $\tan \theta \gg \partial_y h$ ,  $W \propto t^{1/3}$  independently of  $\bar{u}(h)$ ,  $H$  decreases to 0 as  $t^{-2/15}$  for  $\bar{u} \propto h^{3/2}$  (eq. 1) and to  $h_{\text{stop}}$  as  $t^{-1/3}$  for  $\bar{u} \propto h - h_{\text{stop}}$  (eq. 3 for  $h \simeq h_{\text{stop}}$ ).